

The influence of patient centering on CT dose and image noise

Thomas Toth^{a)} and Zhanyu Ge

*CT Systems Engineering W-1140, G.E. Healthcare, General Electric Company,
3000 N. Grandview Boulevard, Waukesha, Wisconsin 53201-0414*

Michael P. Daly

*Electromagnetics Laboratory, Department of Electrical and Computer Engineering,
University of Illinois at Urbana-Champaign, Urbana, Illinois 61801*

(Received 9 October 2006; revised 16 May 2007; accepted for publication 17 May 2007;
published 27 June 2007)

Although x-ray intensity shaping filters (bowtie filters) have been used since the introduction of some of the earliest CT scanner models, the clinical implications on dose and noise are not well understood. To achieve the intended dose and noise advantage requires the patient to be centered in the scan field of view. In this study we explore the implications of patient centering in clinical practice. We scanned various size and shape phantoms on a GE LightSpeed VCT scanner using each available source filter with the phantom centers positioned at 0, 3, and 6 cm below the center of rotation (isocenter). Surface doses were measured along with image noise over a large image region. Regression models of surface dose and noise were generated as a function of phantom size and centering error. Methods were also developed to determine the amount of miscentering using a scout scan projection radiograph (SPR). These models were then used to retrospectively evaluate 273 adult body patients for clinical implications. When miscentered by 3 and 6 cm, the surface dose on a 32 cm CTDI phantom increased by 18% and 41% while image noise also increased by 6% and 22%. The retrospective analysis of adult body scout SPR scans shows that 46% of patients were miscentered in elevation by 20–60 mm with a mean position 23 mm below the center of rotation (isocenter). The analysis indicated a surface dose penalty of up to 140% with a mean dose penalty of 33% assuming that tube current is increased to compensate for the increased noise due to miscentering. Clinical image quality and dose efficiency can be improved on scanners with bowtie filters if care is exercised when positioning patients. Automatically providing patient specific centering and scan parameter selection information can help the technologist improve workflow, achieve more consistent image quality and reduce patient dose. © 2007 American Association of Physicists in Medicine. [DOI: [10.1118/1.2748113](https://doi.org/10.1118/1.2748113)]

I. INTRODUCTION

The impact of image noise and dose has been a topic of interest to medical doctors and physicists since the earliest days of computer tomography (CT).¹ High interest continues to be driven by concern regarding increasing utilization of CT scanners and the corresponding impact on population dose. The relationship between object size, image noise and dose is well understood.^{2,3} Noise is an important clinical factor since it can degrade diagnostic performance and dose is a necessary undesired factor that is inversely related to noise by its square root.

The medical physics community is engaged in educating and informing CT scanner users in practical clinical methods to select appropriate scan parameters that achieve acceptable diagnostic quality with the lowest possible dose.^{4–6} Because of the dominant role of patient size on image noise, automatic tube current modulation (ATCM) has been deployed on modern CT scanners.⁷ ATCM z -axis modulation can help provide predictable image noise to account for patient size attenuation variation. ATCM x/y modulation adjusts the tube current in accordance with patient attenuation asymmetry to achieve a dose advantage without substantially increasing noise.

The bowtie beam shaping filter is another important element in the CT image chain that is provided on modern CT scanners. While tube current modulation adjusts overall x-ray beam intensity in accordance with patient size, the bowtie filter spatially shapes the x-ray field intensity within the scan field of view (SFOV) as shown in Fig. 1. The function of a bowtie filter is to project maximum x-ray to the thickest region of the patient that attenuates the most x-ray and to reduce x-ray intensity where patient attenuation decreases. As a result, bowtie filters reduce dose, but also increase noise especially toward the periphery of the image. Figure 1 shows the normalized beam intensity profiles for the small, medium, and large bowtie filters on the GE LightSpeed VCT scanner.

Modern CT scanners often have more than one bowtie filter that can be used for patient scanning. On GE scanners, the CT technologist selects the filter for the patient indirectly by manually selecting one of several SFOV selections. These selections describe the patient anatomy and size intended to be scanned in general terms such as SMALL BODY, MEDIUM BODY, LARGE BODY, HEAD, etc. The SFOV parameter selects a bowtie filter that produces an x-ray profile consistent with the SFOV description. For example, LARGE BODY would select the filter with the widest field of un-

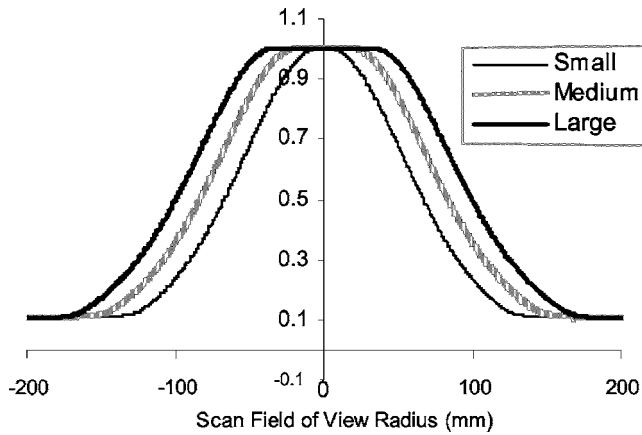


FIG. 1. Normalized x-ray beam intensity profile at 120 kVp as a function of the scan field of view radius for the small, medium and large bowtie beam shaping filters on the LightSpeed VCT.

attenuated x ray. The CT technologist will generally use qualitative criteria to determine which SFOV applies to a given size patient.

Recent studies have theoretically shown the importance of matching a bowtie filter to the object being scanned.^{8,9} A filter that is too flat for the size of the object provides a high dose relative to the noise within the overall image. Conversely, a filter that is too narrowly shaped produces too much noise relative to the dose reduction. These studies have assumed that the object being scanned is properly centered in the scan field of view (SFOV).

From Fig. 2 we would expect miscentering to produce a nonoptimal condition where surface dose increases in the region that moves toward the less attenuating part of the bowtie and noise increases in the region that moves into the more attenuating part of the bowtie. The principal objective of this study was to assess the clinical implications on dose and noise with respect to patient miscentering within the SFOV. To do this, we developed software tools to determine

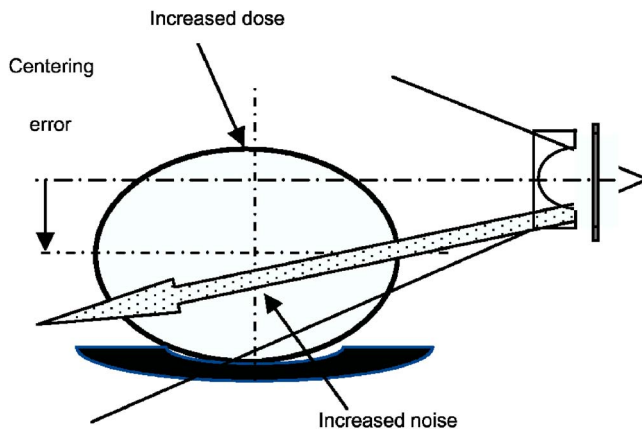


FIG. 2. A patient that is miscentered in the scan field of view can be expected to have degraded bowtie filter performance with an undesired increase in both dose and noise.

TABLE I. Phantoms, dimensions and material.

Symbol	Material	Diam. (cm)
W12.5	Water	12.5
W20	Water	21.5
W25	Water	26.5
W35	Water	36.5
W46	Water	47.5
P48	Polyethylene	48
CTDI16	PMMA	16
CTDI32	PMMA	32
S-CRIS ^a	Tissue Eq.	29.6 × 21.8
L-CRIS ^a	Tissue Eq.	38.4 × 30.8

^aModel 007TE Computerized Imaging Reference Systems, Inc.

miscentering from the patient's scan projection radiograph (scout SPR scan) and to estimate the effects of miscentering on the surface dose and noise.

II. METHODS

A. Phantom dose and noise measurements

Various size and shape phantoms (Table I) were scanned on a GE LightSpeed VCT using each available bowtie shaping filter with an x-ray technique of 120 kV, 8 × 5 mm axial slice collimation and a 1 s gantry rotation period. Phantoms were positioned at 0, 3, and 6 cm below center of rotation (isocenter) on the patient table and also in air for those phantoms with phantom holder mounting capabilities. Scout SPR scans were also obtained for the phantoms with the tube at 12:00 and 3:00 positions (viewed from table side of the gantry).

Axial dose was measured using a standard 10 cm CT pencil chamber on the top, side and bottom surface of the phantoms. The scans were repeated for each position. In addition, peripheral and central doses were measured for the CTDI and CRIS phantoms using the available pencil chamber access holes. Standard deviation (SD) was measured as an indicator of image noise using difference images of repeated scans to remove correlated features and any residual CT number nonuniformities. SD measurements were made for large elliptically shaped region of interest (ROI) representing approximately 80% of the uniform phantom pixel area. The SD for the pixels in the top and bottom halves of the ROI were also independently measured to assess localized changes in noise with miscentering. The measurements were averaged over the eight axial difference images and were divided by the square root of two to account for using difference images.

B. Object size characterization

Since the size and density of the scanned object is a factor that influences dose and noise, we needed an objective metric that could be determined from the patient's scout SPR. The projection area is a parameter already used for z axis (longitudinal) automatic tube current modulation⁷ (automA and smartmA on GE scanners). The projection area is the

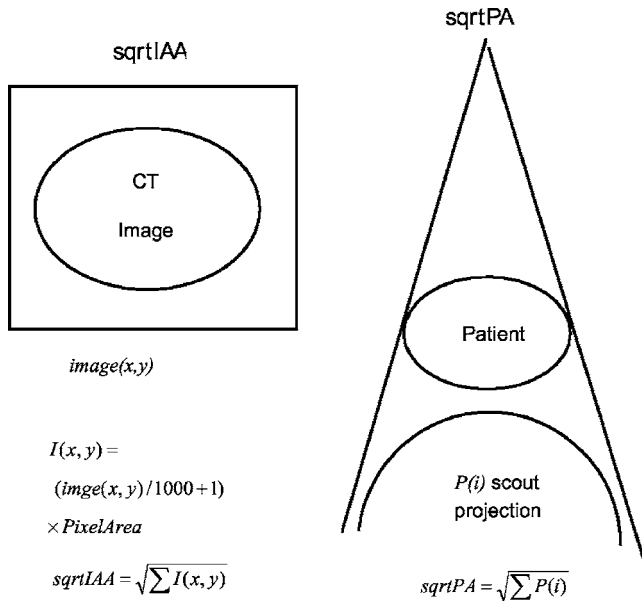


FIG. 3. The size of a scanned object or patient can be characterized in terms of an objective x-ray attenuation metric such as the square root of the image area (sqrtIAA) or the square root of the projection area (sqrtPA). The sqrtIAA is a scanner independent patient attenuation indicator (PAI) that can be determined from the sqrtPA or directly from an axial image.

summation of detector channel data values after natural log and beam hardening corrections and therefore represents a measure of total object attenuation (Fig. 3). The square root of the projection area should therefore correlate with object size.

As a matter of related interest, we also calculated the square root of the image attenuation area (sqrtIAA). This can easily be computed for any dicom axial CT image as shown in Fig. 3. The sqrtIAA is calculated by summing the image pixel values after first converting from HU values to μa values, where μ is the normalized attenuation coefficient relative to water and a is the area per pixel in cm^2 . Thus, the sqrtIAA is a single attenuation metric that is similar to the sqrtPA except for the geometric sampling differences. The sqrtPA is dependent on scanner sampling geometry and patient position but the sqrtIAA is not (assuming the entire object is contained within the image).

C. Automatic patient centering determination

Scout SPR scans of various phantom sizes and center positions were also analyzed in order to determine an algorithm to recommend recentering adjustments to the technologist.

- The raw x-ray projections from a scout SPR acquisition are preprocessed with the customary reference normalization, air calibration, inverse log and beam hardening corrections.
- The preprocessed data are averaged over all views within the valid Z-axis section of the phantom.
- The centroid of the average projection is calculated to determine where attenuation of the object is mainly located relative to the isocenter detector channel.

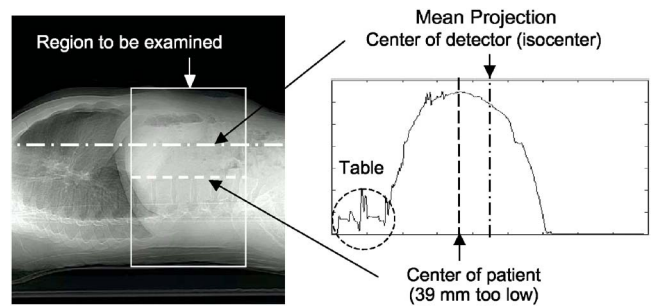


FIG. 4. Example of an adult abdominal patient that is miscentered 39.4 mm below isocenter. The miscentering is calculated from a lateral scout SPR by determining the difference between isocenter and the centroid for the mean projection over the region to be examined. The result is adjusted by a table correction factor that is dependent on sqrtPA of the mean projection.

- The centroid minus the isocenter detector channel can be used to calculate an estimate of the linear error in mm using scanner geometry parameters (detector pitch angle, source to isocenter distance, and source to detector distance).

With the phantom on the table, the centroid gives the position of the combined table and patient attenuation. The goal, however, is to center the patient region excluding the table since an image of the table generally does not have any diagnostic value. Thus, we needed a method to minimize the impact of the table attenuation on the centering report.

- To center only the phantom, we calculated a regression model as a function of sqrtPA for the center of the phantom on the table determined using the centroid minus the true phantom center known from the table elevation readout. The regression model estimates the error due to the presence of the table in the phantom plus table projection data. The table error model is dependent on the sqrtPA since the table is a larger percentage of the total attenuation for smaller objects.
- The estimated error for the table is then subtracted from the overall position indicated by the centroid of object plus table.
- The adjusted centering calculation for the region to be examined is used during patient scanning to predict the table elevation adjustment that is needed to properly center the patient (Fig. 4).

For scout SPR scans with an AP orientation (tube at 6:00 or 12:00), the table attenuation projection is naturally centered and does not substantially affect the centroid calculation for patient centering determination. Thus the table attenuation does not produce a centering error for AP oriented scout SPR scans.

D. Clinical implications

We studied the clinical implications of patient miscentering using laboratory analysis SW called computer assisted parameter selection (CAPS) that was written in the MATLAB programming language (The MathWorks, Inc. Natick, MA).

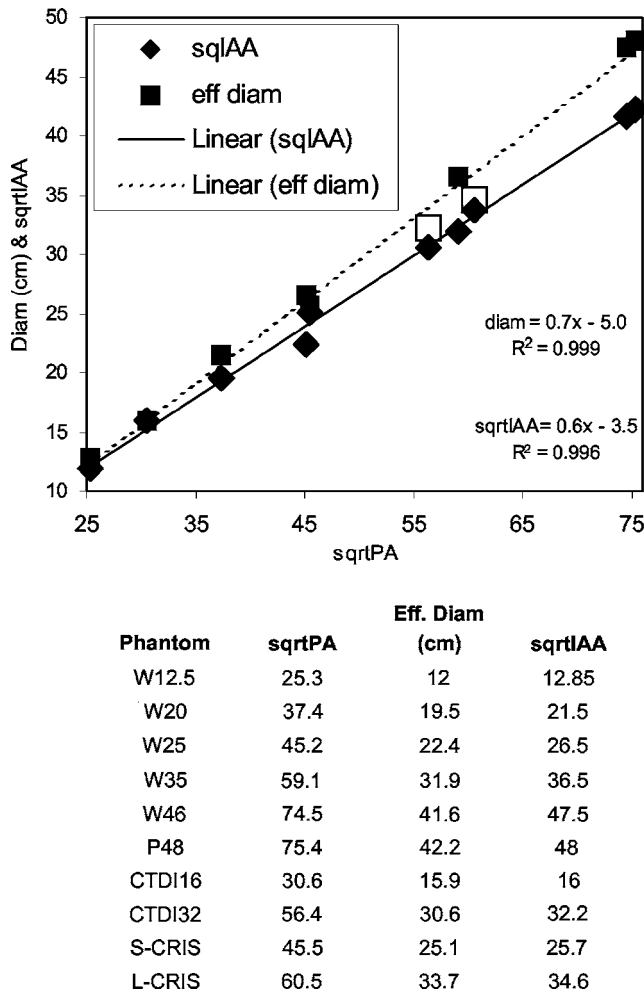


FIG. 5. There is a strong linear relationship of the effective phantom diameter and the sqrtIAA with the sqrtPA. The open boxes identify the L-CRIS and the CTDI32 phantoms that are effective diameter outliers due to density differences. The regression equations were derived from the water phantoms and excluded the phantoms composed of other materials.

CAPS analyzes dicom scout SPR images to determine the projection area using the same algorithm employed by automA in GE LightSpeed scanners. CAPS determines patient miscentering over the region to be imaged using the methods previously described.

In addition, CAPS includes regression models to estimate the surface dose and noise increases due to miscentering. The models are a function of patient size in terms of sqrtPA and miscentering in mm and were determined from the dose and noise measurements using the set of phantoms in Table I.

We obtained a total of 549 AP and lateral scout SPR images for 273 anonymous adult body patients from previously completed clinical studies provided by a variety of institutions. Our analysis was completely retrospective and therefore did not influence any clinical patient examinations.

The data set included 254 female and 295 male images with adult ages ranging from 21 to 102 years. Several pediatric images of males with ages ranging between 6 and 18 years were also included in the image set.

The scout SPR images were analyzed using CAPS to de-

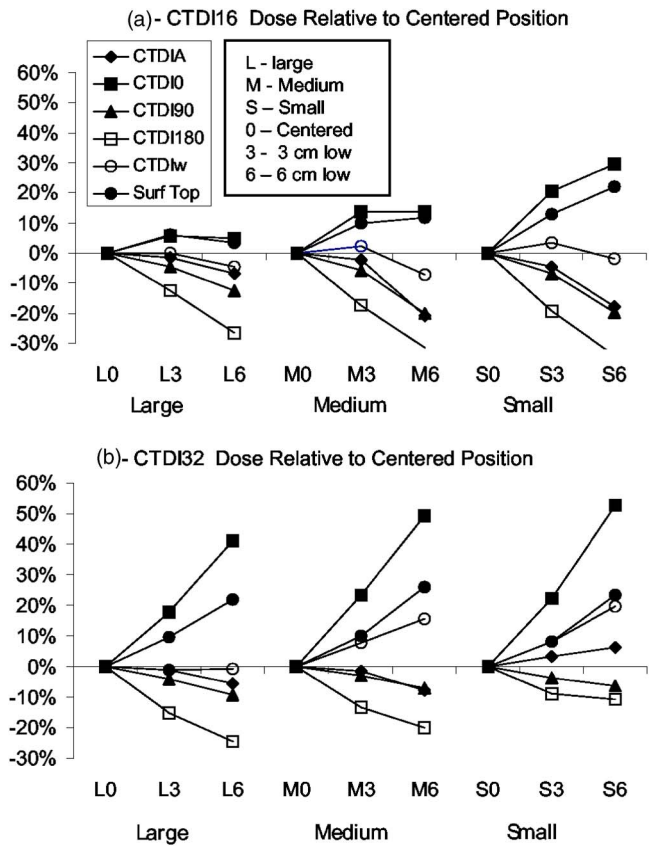


FIG. 6. Percent dose change relative to a centered phantom for the CTDI16 and CTDI32 phantoms with each filter with the phantoms centered at 0, 3, and 6 cm below isocenter. The CTDI suffix definitions are: A—center, 0—top, 90—side, 180—bottom, and W—weighted. CTDI0 and Surf Top dose changes have a similar trend while the CTDIw is largely unaffected since the top and bottom peripheral dose changes tend to cancel.

termine, the mean sqrtPA of the abdominal region, the required centering adjustment, and an estimate of the surface dose and noise increases.

III. RESULTS

A. Size characterization

Plots of the sqrtIAA and effective diameter as a function of sqrtPA are shown in Fig. 5. The effective diameter is the mean diameter (average of the major and minor axis for non-circular phantoms). A linear regression using the water phantoms accurately relates the sqrtPA to effective diameter and sqrtIAA ($R^2 > 0.99$). The open boxes identify the L-CRIS and the CTDI32 phantoms that are effective diameter outliers due to shape and density differences. The nonwater phantoms were excluded from the regression. Figure 5 shows that the sqrtPA or sqrtIA is an accurate metric for phantom size with some expected error for phantoms with densities different than water. The errors due to density differences are somewhat minimized by the square root operation. However, dimensional size was not used in any of our prediction models and the relationship of sqrtPA with size is shown here only for illustration purposes.

20 cm water phantom noise contour plots vs filter and miscentering

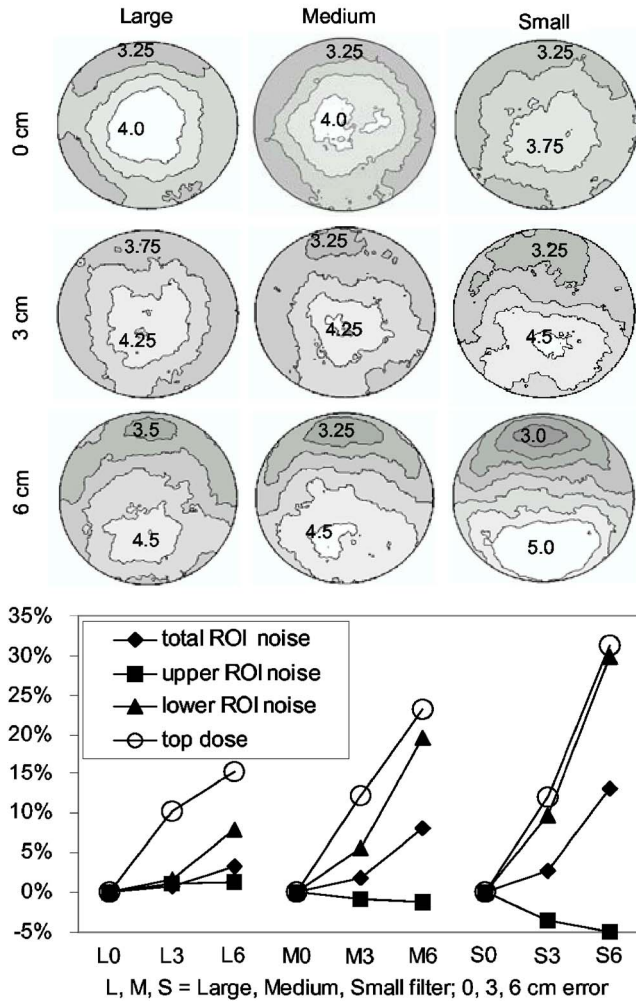


FIG. 7. The percent change in image noise and top surface dose increase with miscentering for the 20 cm water phantom. Noise increases with miscentering especially in the lower phantom region where bowtie attenuation increases with miscentering. The contour plots visually show how noise is distributed within the phantom. The lower chart provides the percent top surface dose, total ROI area noise, the upper half ROI noise and lower half ROI noise where the ROI is circular over 80% of the water region.

B. Dose and noise with centering error

Figure 6 shows plots of the percent dose change relative to the centered condition for the 16 and 32 cm CTDI phantoms at positions of 0, 3, and 6 cm below isocenter for each bowtie filter (large, medium and small). In general, the surface dose at the top of the CTDI phantoms (CTDI-0) increases while the dose at the bottom decreases as the phantom is miscentered lower. Since the increase and decrease tend to be balanced, the net effect on the overall CTDIw dose is negligible when calculated using the peripheral mean. The top peripheral dose (CTDI-0) and top surface dose disturbances are generally enhanced with the smaller bowtie filters. For example, at 6 cm below isocenter, the top peripheral

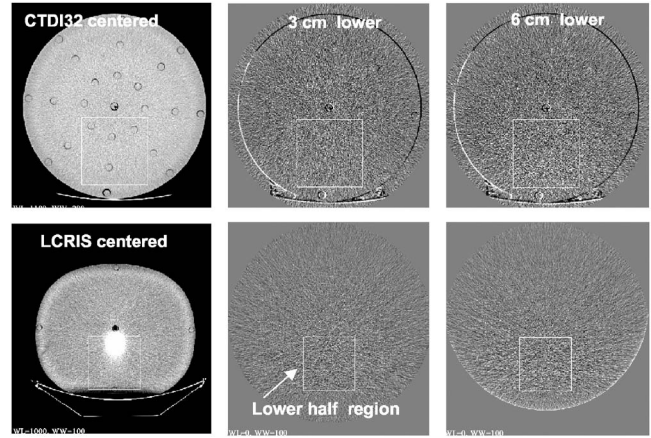


FIG. 8. Example CTDI32 and LCRIS difference image noise with miscentering. Note substantial noise increase that occurs in the lower portion of the phantom within the region identified by the white square.

(CTDI-0) dose of the 16 cm CTDI phantom [Fig. 6(a)] increases by 5%, 12% and 32% for the large, medium, and small bowtie filters respectively.

With miscentering, the top surface dose on the 16 cm CTDI phantom (CTDI16) closely follows the CTDI-0 peripheral dose. The top surface dose for the 32 cm CTDI phantom (CTDI32) follows a similar trend with approximately one half the intensity. The CTDI 90° peripheral dose (CTDI90) does not appreciably change.

The contour plots in Fig. 7 show how noise is distributed within the 20 cm water phantom (W20) as the phantom is miscentered with each bowtie filter. The lower chart provides the percent change in top surface dose, the total ROI area noise, the upper half ROI noise and the lower half ROI noise where the ROI is a circular region covering approximately 80% of the water area of the phantom.

As expected, noise change with miscentering is least sensitive with the large bowtie. With a 6 cm centering error using the large bowtie filter, image noise increases only about 3% over the total image ROI area and 8% in the lower ROI half. With a 6 cm error using the medium filter, image noise increases by 8% overall and 20% in the lower half ROI. Miscentering has the greatest effect on noise distribution with the small filter. Overall ROI noise increases by 3% and 13% while the bottom half ROI noise increases by 10% and 30% with 3 and 6 cm errors, respectively. With the medium and small filters, there is a slight decrease in noise in the top half image ROI (1% and 5%, respectively).

Figure 8 shows a visual example of the how noise increases with miscentering in the lower section of the image for larger size phantoms with the body bowtie filter. Figure 9 shows dose and noise charts for all the phantoms for which the large bowtie filter is likely to be used and is intended to represent the attenuation range of typical adult abdominal scanning. The table at the bottom of Fig. 9 gives the percent surface dose increase assuming that the lower region noise has been compensated by increasing the dose by an amount proportional to the square of the noise increase. Quadratic regressions for surface dose, noise and noise adjusted surface

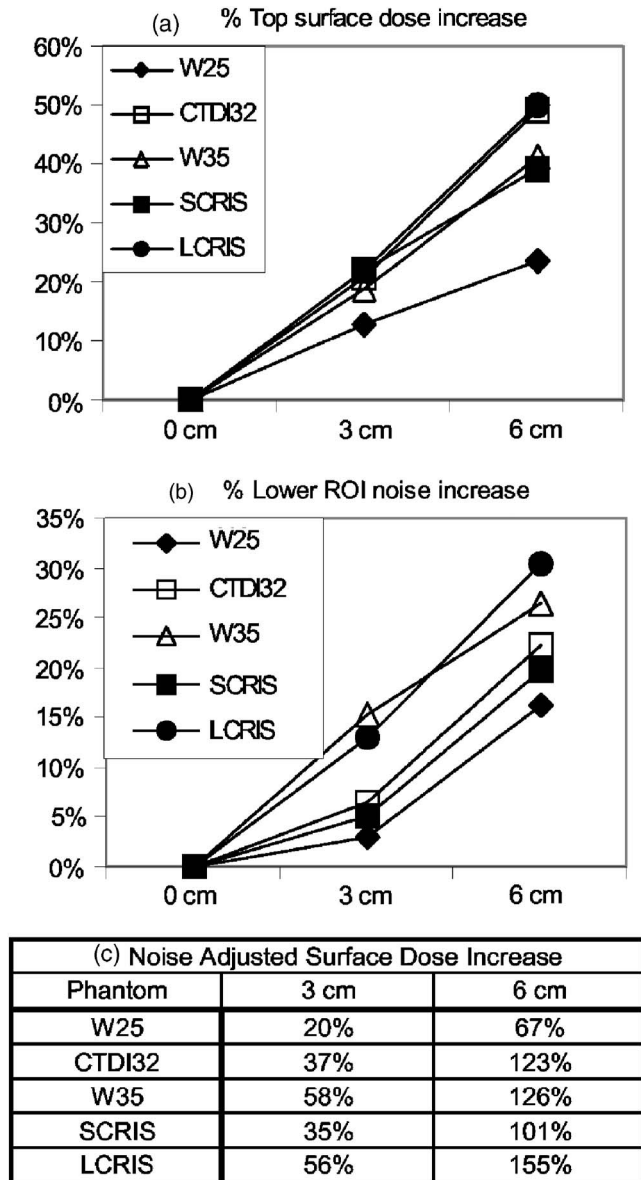


FIG. 9. Shows the top surface dose, lower ROI region noise and noise adjusted surface dose versus centering error for the larger phantoms with the large bowtie filter. The noise adjusted surface dose assumes the dose is increased to maintain the original lower ROI region noise for the centered phantom.

dose as a function of sqrtPA and miscentering provide models to assess clinical dose implications. These regression models have R² values of 0.968, 0.987 and 0.992 for lower ROI region noise, surface dose and noise adjusted dose, respectively.

C. Centering adjustment estimates

The errors using the centroid calculation when the phantoms are scanned in air (on a phantom holder) are shown in Fig. 10(a). The large errors for the W46 and P48 phantom occur for centering positions when part of the phantom is outside the scan field of view. Otherwise the mean calcula-

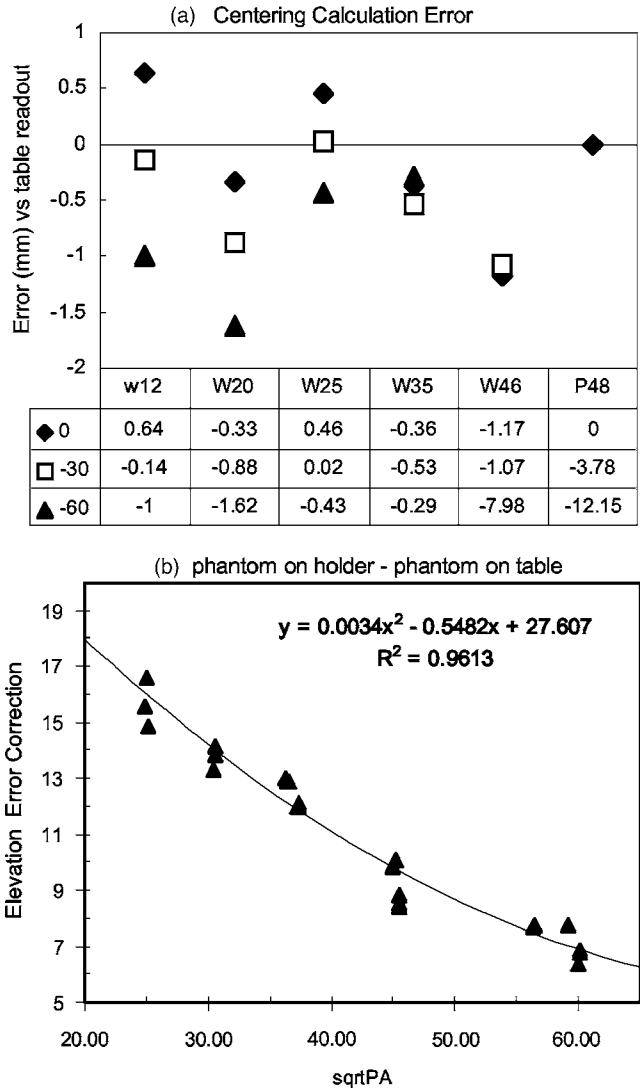


FIG. 10. Centering estimation errors when using the centroid method. Chart A is the calculated error relative to the table height read for phantoms scanned in air. Chart B is the compensation required to minimize the effect of the table when phantoms are scanned on the patient table.

tion errors are -0.13, 0.52, and -1.02 mm of the actual position as indicated by the scanner table elevation readout for 0, 3, and 6 cm scan centering positions.

Figure 10(b) shows the centering calculation difference from the table elevation readout as a function of sqrtPA with the phantom on the holder minus the phantom on the table. This difference represents the correction factor required to compensate for the table. The table correction factor is estimated using the regression model shown in Fig. 10. Note that the effect of the table diminishes as sqrtPA increases. This occurs since the table is a smaller percentage of the total object attenuation and therefore has less of an effect on the centroid.

D. Clinical implications of patient size and centering

The retrospective CAPS analysis of the 549 patient scout SPR scans, shown in Fig. 11, indicated that the mean sqrtPA

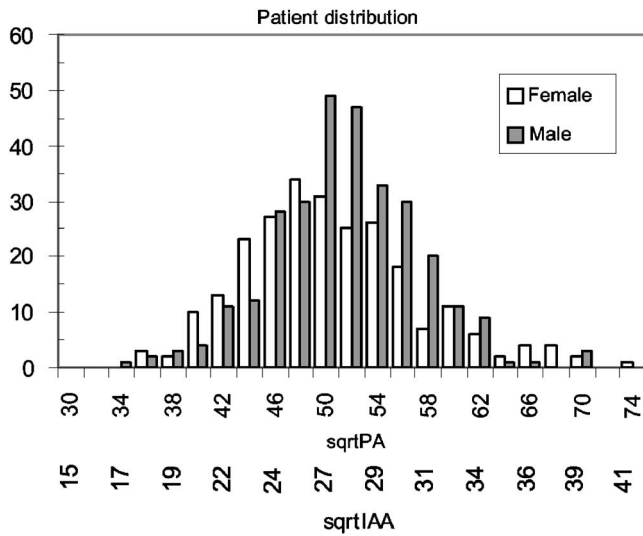


FIG. 11. Size distribution of adult abdominal patients in terms of the mean sqrtPA and sqrtIAA.

over the abdominal region ranged from a low of 34 to a high exceeding 74 (sqrtIAA range of 17–41). The mean sqrtPA was 49.7 for females and 50.3 for males. The mean adult abdominal patient has a sqrtIAA of 26.5 and has overall attenuation characteristics similar to a 30 cm water phantom using the relationships shown in Fig. 5

Clinical patient centering results are shown in Fig. 12. A distribution of errors in elevation and lateral positioning is shown in Fig. 12 chart (a). Charts (b) and (c) of Fig. 12 show scatter plots of elevation and lateral positioning errors as a function of patient size in terms of the mean abdominal sqrtPA.

Lateral positioning errors range from -2.9 to 3.3 cm with a mean of 0.0 cm. Elevation errors range from -6.6 to 3.4 cm with a mean error of -2.3 cm. A substantial number of patients (74%) were miscentered in elevation by more than 1 cm. Many patients (22%) were miscentered by more than 3 cm. The elevation scatter plot (b) shows a weak tendency for smaller patients to be miscentered by a larger amount than larger patients. The lateral scatter plot (c) does not reveal any similar tendency with patient size.

The charts shown in Fig. 13 were generated using the regression models for dose and noise versus the patient mean abdominal sqrtPA and centering error values for each patient scout SPR. Chart (a) shows the percent of patients for which the associated increase in dose and noise is equal or greater than the value shown on the abscissa. The mean increase in noise, surface dose, and noise adjusted surface dose is 7%, 15%, and 33%, respectively. Noise, surface dose, and noise adjusted surface dose increase by a minimum of 5%, 15% and 25%, respectively, for 50% of patients. These values increase to 12%, 26%, and 55%, respectively, for 20% of patients. The noise adjusted surface dose is more than doubled for 4% of patients (off the chart).

The scatter plots in Figs. 13(b)–13(d) show the distribution of patient dose and noise increases versus centering er-

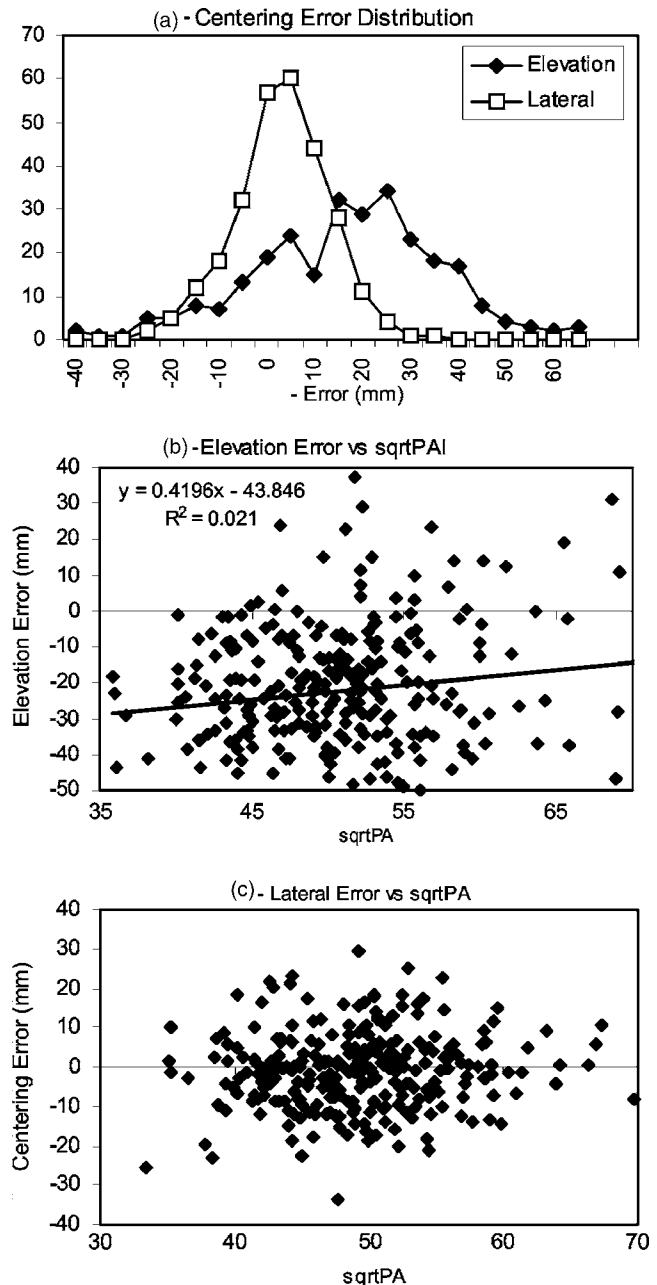


FIG. 12. Distribution of patient centering errors in elevation and lateral positioning. A distribution of errors is shown in chart (a). Charts (b) and (c) show scatter plots of elevation and lateral positioning errors as a function of mean abdominal sqrtPA. There appears to be a weak tendency for smaller patients to be miscentered in elevation more than large patients.

ror. The spread in values occurs due to the impact of miscentering on the dose and noise increase with patient size.

IV. DISCUSSION

A. Patient size characterization

We successfully employed the sqrtPA as a patient size factor to predict and remove the influence of the table on patient centering and to estimate dose and noise. However, we believe that the sqrtIAA may be a more important discovery as a convenient way to characterize patient size in

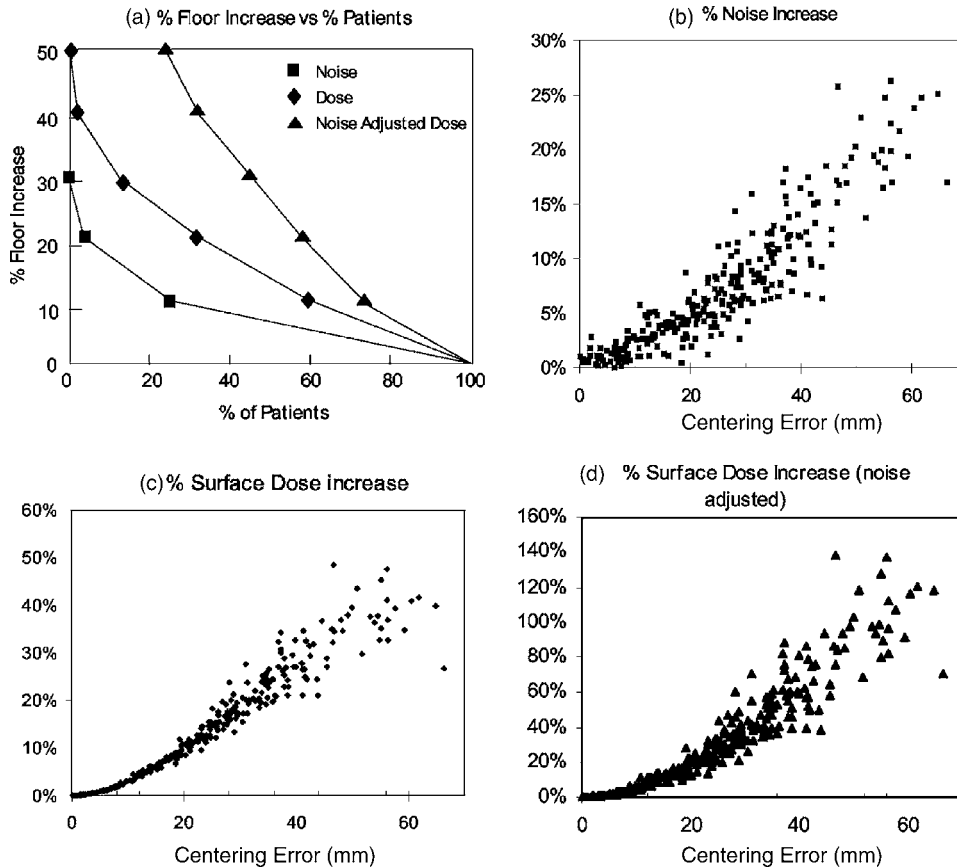


FIG. 13. Clinical implications of miscentering on dose and noise. Chart (a) shows the percent of patients with a dose and noise increase equal or greater than the value shown on the abscissa. Charts (b, c, and d) are scatter plots for the noise, surface dose, and noise adjusted surface dose, respectively.

terms of overall x-ray attenuation. There may be situations where the sqrtIAA might be a more useful diagnostic clinical indicator than the patient weight, body mass index or girth measurements that are currently used as factors for some statistical medical relationships. The sqrtIAA could be routinely reported with the CT image to allow the medical community to explore its potential use as a medical or diagnostic indicator.

sqrtIAA is independent of scanner make and model and could be reasonably accurate. Some care would be required to minimize calculation errors since direct calculations from an image would exclude attenuation outside the image DFOV and calculations obtained from a scout SPR scan would be affected by centering and tube orientation. The best calculation method might be to use a scaled version of the sqrtPA that is obtained from an average of the projections used to create the CT image.

B. Clinical implications of patient miscentering

Adult body patient miscentering in elevation was surprisingly prevalent, ranging from -6.6 to 3.4 cm with a mean of -2.3 cm. Body patients are generally scanned supine and table elevations tend to be distributed below isocenter. This means that the dose absorbed by dose sensitive anterior organs, such as the breast, will be increased. This increase may be even higher since image noise is also adversely affected by miscentering and thereby could encourage the use of higher x-ray technique factors.

Since patients are generally wider in the lateral axis than the transverse axis, the effect on noise due to low miscentering can be especially intense since attenuation in the long patient axis adds to the bowtie attenuation. In some extreme cases, the resulting noise adjusted surface dose increase can be more than doubled [Fig. 13(d)].

A limitation of our study recognizes that clinical dose is very patient dependent and should be determined in terms of a human dose metric such as effective dose. Our study extrapolated surface dose and noise with miscentering to clinical patients based on measurements in simple phantoms. As a result, the actual effective dose increases to the CT patient population may be different than we presented. Future work is needed to explore these clinical relationships more carefully. However, the phantom results provide strong evidence that dose and noise can be expected to increase with miscentering in clinical patients.

It is, therefore, critically important that technologists make an extra effort to center patients in elevation as carefully as possible. This could be done using graphical methods from the scout SPR image. For example, when a patient is miscentered, many technologists use the lateral scout SPR, to graphically determine the DFOV and to offset the image reconstruction to center the images. A better choice would be to use the graphical miscentering measurement to recenter the patient before continuing with the transverse scout SPR and/or the CT exam. In this way the patient would be prop-

erly centered in the SFOV to achieve dose and noise advantages in addition to obtaining patient anatomy that is centered in the image DFOV.

Another approach to improve patient centering is to calculate and provide the centering information to the user from the lateral scout SPR. This approach was successfully used in a clinical study¹⁰ that employed prototype SW to calculate clinical patient centering as discussed in the Methods section. A lateral scout SPR is required for automatic elevation centering calculations. A very high percentage of institutions seem to use both an AP and a lateral scout SPR scans for most procedures so an extra scan for centering is not usually needed. The lateral scout SPR scan could be an ultralow dose or sampled at periodic patient locations for institutions where the lateral scout is not normally taken.

Our analysis of clinical scout SPR data indicated that lateral patient positioning does not have the systemic centering offset inherent in elevation positioning (0.1 cm lateral mean versus -2.3 cm elevation mean). Lateral centering may be easier to achieve because the sides of table provide a good visual reference for the technologist, whereas there is no such visual reference for elevation. The tendency for low table elevations may result from the natural need to lower the table to allow the patient to mount and dismount more easily. Although there are insufficient samples to make a conclusive statement, the data seem to suggest that small patients may be centered even lower than larger patients [Fig. 12(b)].

V. CONCLUSIONS

The impact of patient miscentering on dose and image quality deserves increased attention in clinical practice. We have shown that patient miscentering may substantially increase image noise and surface dose. As a result, technologists should be encouraged to improve patient centering, especially in elevation. We have shown that a lateral scout SPR scan can provide patient centering adjustment information for the technologist. CT technologists face a substantial chal-

lenge in selecting the appropriate parameters for a CT scan. Methods to automatically select scan parameters that are appropriately tailored to the patient and to provide centering assistance for the technologist could help improve scan quality and reduce patient dose.

ACKNOWLEDGMENT

The authors would like to acknowledge Laura Tuszynski, an intern at GE Healthcare, who helped organize and finalize the CAPS software that we used to retrospectively analyze patient scout SPR scan images.

^{a)}Electronic mail: thomas.toth@ge.com

¹K. M. Hanson, "Detectability in computed tomographic images," *Med. Phys.* **6**, 441–451 (1979).

²M. J. Siegel, B. Schmidt, D. Bradley, C. Suess, and C. Hildebolt, "Radiation dose and image quality in pediatric CT: Effect of technical factors and phantom size and shape," *Radiology* **233**, 515–522 (2004).

³E. Nickoloff, A. Dutta, and Z. Lu, "Influence of phantom diameter, kVp and scan mode upon computed tomography dose index," *Med. Phys.* **30**, 395–402 (2003).

⁴C. H. McCollough, M. R. Bruesewitz, and J. M. Kofler, Jr., "CT dose reduction and dose management tools: Overview of available options," *Radiographics* **26**, 503–512 (2006).

⁵W. Huda, K. A. Liberman, J. Chang, and M. Roskopf, "Patient size and x-ray technique factors in head computed tomography examinations," *Med. Phys.* **31**, 595–601 (2004).

⁶M. J. Siegel, B. Schmidt, D. Bradley, C. Suess, and C. Hildebolt, "Radiation dose and image quality in pediatric CT: Effect of technical factors and phantom size and shape," *Radiology* **233**, 515–521 (2004).

⁷M. K. Kalra, M. M. Maher, T. L. Toth, B. Schmidt, B. L. Westerman, H. T. Morgan, and S. Saini, "Techniques and applications of automatic tube current modulation for CT," *Radiology* **233**, 649–657 (2004); published online before print as 10.1148/radiol.2333031150

⁸T. L. Toth, I. T. Toth, E. Cesmeli, A. Ikhlef, and T. Horiuchi, "Image quality and dose optimization using novel x-ray source filters tailored to patient size," *Proc. SPIE* **5745–5734**, 283–291 (2005).

⁹M. Harpen, "A simple theorem relating noise and patient dose in computed tomography," *Med. Phys.* **26**, 2231–2234 (1999).

¹⁰J. Li, M. Kalra, T. Toth, U. Udayasanka, J. Seamans, and W. Small, "Automatic patient centering for multisection CT: Effect on radiation dose and image quality," *AJR, Am. J. Roentgenol.* **188**, 547–552 (2007).